IEEE Photonics Journal
An IEEE Photonics Society Publication



# Design of Few-Mode Fibers for Mode-Division Multiplexing Transmission

Volume 5, Number 6, December 2013

**Motoki Kasahara**
**Kunimasa Saitoh, Member, IEEE**
**Taiji Sakamoto**
**Nobutomo Hanzawa**
**Takashi Matsui**
**Kyozo Tsujikawa**
**Fumihiko Yamamoto**
**Masanori Koshiba, Fellow, IEEE**

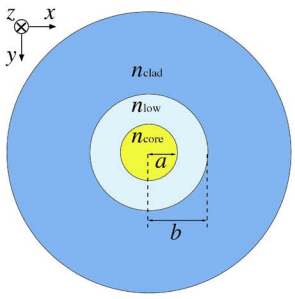


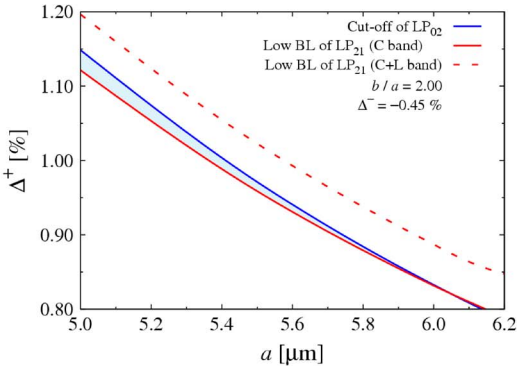


DOI: 10.1109/JPHOT.2013.2292365
1943-0655 © 2013 IEEE

# Design of Few-Mode Fibers for Mode-Division Multiplexing Transmission

**Motoki Kasahara,[1] Kunimasa Saitoh,[1] *Member, IEEE*, Taiji Sakamoto,[2] Nobutomo Hanzawa,[2] Takashi Matsui,[2] Kyozo Tsujikawa,[2] Fumihiko Yamamoto,[2] and Masanori Koshiba,[3] *Fellow, IEEE***

[1]Graduate School of Information Science and Technology, Hokkaido University, Sapporo 060-0814, Japan
[2]Access Network Service Systems Laboratories, NTT Corporation, Tsukuba 305-0805, Japan
[3]Career Center, Hokkaido University, Sapporo 060-0808, Japan

*DOI: 10.1109/JPHOT.2013.2292365*
*1943-0655 ©2013 IEEE*

Manuscript received October 11, 2013; revised November 5, 2013; accepted November 13, 2013. Date of publication November 21, 2013; date of current version December 2, 2013. Corresponding author: M. Kasahara (e-mail: kasahara@icp.ist.hokudai.ac.jp).

**Abstract:** We investigate the fiber parameters that meet the design conditions for low bending loss and an effectively few-mode operation on few-mode fibers with a step-index profile and a W-shaped refractive index profile for mode-division multiplexing transmission. We also clarify the limits of effective area enlargement and the difference of the effective index while satisfying the design conditions.

**Index Terms:** Mode-division multiplexing, few-mode fiber, effective area, difference of the effective index.

## 1. Introduction

Since the data traffic continues to increase rapidly, large transmission capacity will be highly required for optical fiber communication systems. As one of the spatial multiplexing techniques, mode-division multiplexing (MDM) transmission has been attracted as new generation optical fiber communication systems in order to realize large transmission capacity. Many MDM transmission systems using few-mode fibers (FMFs) have been proposed [1]–[4]. Additionally, enlarging the effective area $(A_{\mathrm{eff}})$ is beneficial in reducing the nonlinear effects which degrade the transmission characteristics. Several fiber designs with large $A_{\mathrm{eff}}$ have also been proposed [5], [6]. However, a study on the limits of $A_{\mathrm{eff}}$ enlargement on FMFs for MDM transmission is still not sufficient.

In MDM transmission, the crosstalk by mode coupling is also the subject of further study. The crosstalk between propagation modes can be compensated by multiple input multiple output (MIMO) digital signal processing (DSP), but the complexity and power consumption of the MIMO-DSP increases with getting higher the differential mode delay (DMD). Therefore, using the graded-index FMFs with low DMD is the preferred approach [7], [8]. However, detailed design and precise fabrication process are required to realize desired characteristics. In contrast, by increasing the difference of the effective index $(\Delta n_{\mathrm{eff}})$ between propagation modes, it is possible to avoid the mode coupling. Hence, using the step-index FMFs with large $\Delta n_{\mathrm{eff}}$ is the second preferred approach [9]. We adopt the second preferred approach, which is using the step-index profile and the W-shaped index profile due to the ease of design and fabrication.

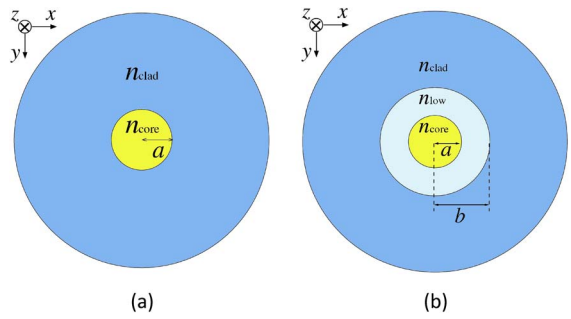


Fig. 1. Schematic cross sections of (a) SIF and (b) WIF.

In regards to the number of propagation modes, Ref. [9] supports four-Linearly Polarized (LP)-mode such as $LP_{01}$, $LP_{11}$, $LP_{21}$, and $LP_{02}$. However, both $LP_{01}$ and $LP_{02}$ modes have a field distribution having a peak in the center of the core. Therefore, in addition to the mode coupling in transmission fiber, the mode conversion occurs at the connection part. Furthermore, the $\Delta n_{\text{eff}}$ between $LP_{21}$ and $LP_{02}$ modes is small.

In this paper, we investigate the fiber parameters that support two- or three-LP-mode under constraints on the bending characteristics of the modes, the limits of $A_{\text{eff}}$ enlargement, and the $\Delta n_{\text{eff}}$. Through detailed numerical simulations based on the finite-element method (FEM) [10], we find that two-mode W-shaped-index fiber (WIF) can push the $A_{\text{eff}}$ limit to much larger values as compared to two-mode step-index fiber (SIF). Additionally, we also show that three-mode SIF cannot meet design conditions, but WIF realizes three-mode transmission.

## 2. Core Design

Schematic cross sections of SIF and WIF are shown in Fig. 1(a) and (b), respectively. The SIF's parameters are the core radius $a$, the refractive index of the core $n_{\text{core}}$, and the refractive index of the cladding $n_{\text{clad}}$. The WIF structure is characterized by three step-index areas, with a low refractive index region surrounding the core region. Such an area is characterized by radius $b$ and refractive index $n_{\text{low}}$. Here, the relative refractive index difference between the core and the cladding is defined as $\Delta^{+} = (n_{\text{core}}^2 - n_{\text{clad}}^2)/(2n_{\text{core}}^2)$, between the low refractive index region and the cladding is defined as $(\Delta^{-} = (n_{\text{low}}^2 - n_{\text{clad}}^2)/(2n_{\text{low}}^2)$, where the background material is assumed to be silica and its refractive index is calculated with Sellmeier equation.

## 3. Two-Mode Fiber Design

### 3.1. Design Condition

We investigate the region satisfying design conditions for two-LP-mode transmission over the C + L band from 1530 nm to 1625 nm. Here, we clarify the effective region by using not the normalized frequency $V$ [9] but the difference of the bending loss (BL). There are two requirements to ensure two-mode transmission. The first requirement is the elimination of the unexpected modes such as $LP_{21}$ and $LP_{02}$ modes. In order to guarantee the two-mode operation, the BL of $LP_{21}$ mode, which is the high-order mode next to $LP_{11}$ mode, is required to be larger than 1 dB/m at 1530 nm when the bending radius equals 140 mm. The BL includes the leakage loss. The second is the low BL of the propagation modes such as $LP_{01}$ and $LP_{11}$ modes. In reference to ITU-T recommendations G.654, the BL of $LP_{11}$ mode, which is one of the propagation modes, is required to be less than 0.5 dB/100 turns at 1625 nm when the bending radius equals 30 mm [11]. In this paper, we refer to not ITU-T recommendations G.652 but G.654 because we assume the cut-off shifted fibers with 1550 nm central wavelength.

Fig. 2 shows structural parameter dependence of design conditions in two-mode (a) SIF and (b) WIF with normalized radius of the low refractive index region $b/a = 1.50$ and the relative refractive

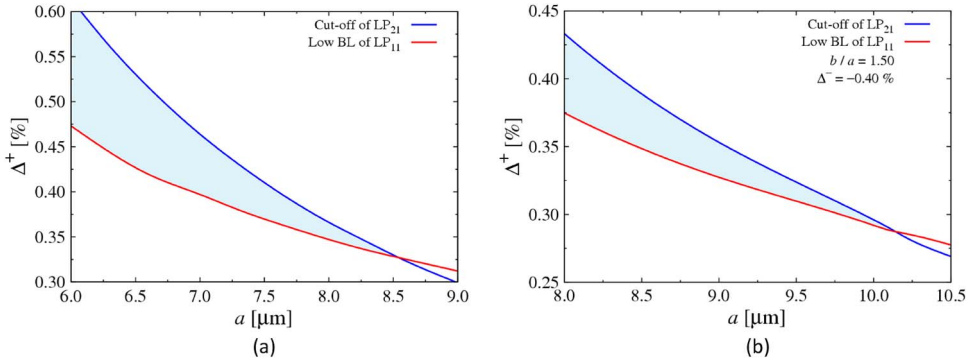


Fig. 2. Structural parameter dependence of design conditions in two-mode (a) SIF and (b) WIF.

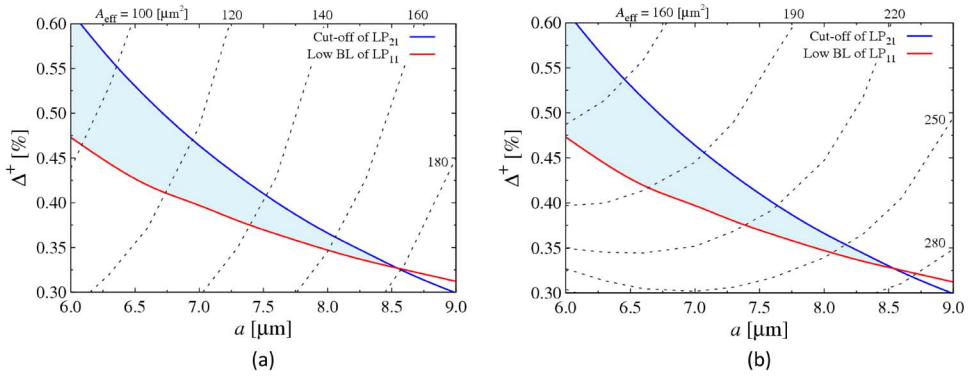


Fig. 3. Structural parameter dependence of $A_{\text{eff}}$ of (a) $LP_{01}$ and (b) $LP_{11}$ modes at 1550 nm.

index difference between the low refractive index region and the cladding $\Delta^- = -0.40\%$, respectively. The solid blue curve indicates that the BL of $LP_{21}$ mode equals 1 dB/m. The BL of $LP_{21}$ mode is larger than 1 dB/m below the blue curve. Therefore, the cut-off of $LP_{21}$ condition is satisfied below the blue curve. The solid red curve indicates that the BL of $LP_{11}$ mode equals 0.5 dB/100 turns. The BL of $LP_{11}$ mode is less than 0.5 dB/100 turns above the red curve. Therefore, the low BL of $LP_{11}$ condition is satisfied above the red curve. Additionally, the BL of $LP_{01}$ mode is approximately one ten-thousandth compared to that of $LP_{11}$ mode in two-mode SIF and WIF. Therefore, both propagation modes are low BL in the region satisfying design conditions. From Fig. 2(a), we find that core radius of approximately 8.5 $\mu$m is achievable in two-mode SIF. This value is nearly double than that of the conventional single-mode SIF. From Fig. 2(b), when we fix $b/a = 1.50$ and $\Delta^- = -0.40\%$, we find that core radius of approximately 10.2 $\mu$m is achievable in two-mode WIF. This value is larger than that of two-mode SIF.

### 3.2. Limit of $A_{\text{eff}}$ Enlargement

Fig. 3 shows variation of $A_{\text{eff}}$ of (a) $LP_{01}$ and (b) $LP_{11}$ modes at 1550 nm as a function of the core radius $a$ and the relative refractive index difference between the core and the cladding $\Delta^+$ in two-mode SIF. The solid blue and red curves are defined as before. From Fig. 3(a) and (b), we find that $A_{\text{eff}}$ of much larger than 100 $\mu m^2$ can be realized for both propagation modes under satisfying design conditions. The limits of $A_{\text{eff}}$ enlargement of $LP_{01}$ and $LP_{11}$ modes are 181 $\mu m^2$, 275 $\mu m^2$, respectively.

In WIF, we need to control $b/a$ so that the core radius becomes maximum. The enlargement of the core radius leads to the enlargement of $A_{\text{eff}}$. We investigate the maximum core radius under satisfying design conditions when $b/a$ varies from 1.00 to 2.25. Fig. 4(a) shows structural parameter

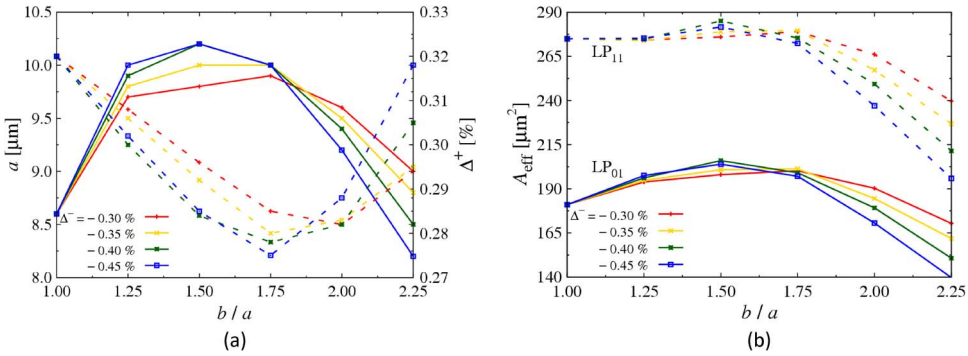


Fig. 4. (a) Structural parameter to satisfy design conditions for two-mode WIF. (b) Max $A_{\text{eff}}$ of $LP_{01}$ and $LP_{11}$ modes at 1550 nm.

to satisfy design conditions for two-mode WIF. The solid lines indicate the upper limits of the core radius $a$. The dashed lines indicate the lower limits of $\Delta^+$. From Fig. 4(a), if we fix $\Delta^- = -0.30$ and $-0.35\%$, the core radius becomes maximum when $b/a = 1.75$, whereas we fix $\Delta^- = -0.40$, $-0.45\%$, the core radius becomes maximum when $b/a = 1.50$. Here, the structure of $b/a = 1.00$ is corresponding to SIF. Therefore, we find that the core radius of two-mode WIF is larger than that of two-mode SIF. Fig. 4(b) shows the maximum $A_{\text{eff}}$ of $LP_{01}$ and $LP_{11}$ modes at 1550 nm as a function of $b/a$ in two-mode WIF. The solid and dashed lines indicate the maximum $A_{\text{eff}}$ of $LP_{01}$ and $LP_{11}$ modes, respectively. From Fig. 4(a) and (b), when the structural parameters are set to $b/a = 1.50$, $\Delta^- = -0.40\%$, $a = 10.2$ $\mu$m, and $\Delta^+ = 0.28\%$, the limits of $A_{\text{eff}}$ enlargement of $LP_{01}$ and $LP_{11}$ modes, are 206 $\mu m^2$, 285 $\mu m^2$, respectively. This maximum value is larger than that of two-mode SIF in the region satisfying design conditions. However, fibers with large $A_{\text{eff}}$ are known to be micro-bending sensitive. For instance, Ref. [12] indicates that micro-bending loss of the SIF with $A_{\text{eff}}$ of 160 $\mu m^2$ is larger than 100 dB/km. Therefore, Ref. [12] also indicates that trench-assisted profiles reduce the micro-bending loss to one tenth compared to the SIF. Additionally, Ref. [13] proposes that fibers with air-holes around the fiber edge suppress the micro-bending loss. From these viewpoints, the limit of $A_{\text{eff}}$ enlargement in consideration of the micro-bending loss is a future work.

### 3.3. Effective Index Difference $\Delta n_{\text{eff}}$

Other characteristic to be considered for FMFs is the mode coupling between propagation modes. Mode coupling depends on a lot of factors, including mode profiles and fiber fabrication. It is known that the large $\Delta n_{\text{eff}}$ minimizes the mode coupling. Ref. [14] proposes $\Delta n_{\text{eff}}$ of 0.0005 for the minimum value. In contrast, Ref. [15], [16] indicate that the mode couplings of the fibers with $\Delta n_{\text{eff}}$ of 0.0013, 0.0028 are 18.2 dB for 500 m $(3.64 \times 10^{-2}$ dB/m), 25 dB for 30 km $(8.33 \times 10^{-4}$ dB/m), respectively. Fig. 5 shows variation of $\Delta n_{\text{eff}}$ at 1550 nm between $LP_{01}$ and $LP_{11}$ modes in two-mode (a) SIF and (b) WIF with $b/a = 1.50$ and $\Delta- = -0.40\%$ as a function of the core radius $a$ and $\Delta^+$. The solid blue and red curves are defined as before. From Fig. 5(a) and (b), we can see that the $\Delta n_{\text{eff}}$ in two-mode SIF and WIF are more than approximately 0.0016, 0.0012, respectively. There is a trade-off between $\Delta n_{\text{eff}}$ and $A_{\text{eff}}$. Therefore, we should chose the structure to satisfy desired conditions of $\Delta n_{\text{eff}}$ or $A_{\text{eff}}$.

## 4. Three-Mode Fiber Design

### 4.1. Design Condition

We investigate the region satisfying the design conditions for three-LP-mode transmission over the C band from 1530 nm to 1565 nm or C + L band from 1530 nm to 1625 nm. The design conditions are the cut-off of $LP_{02}$ and the low BL of $LP_{21}$. The cut-off of $LP_{02}$ means that the BL of $LP_{02}$ mode, which is the high-order mode next to $LP_{21}$ mode, is required to be larger than 1 dB/m at

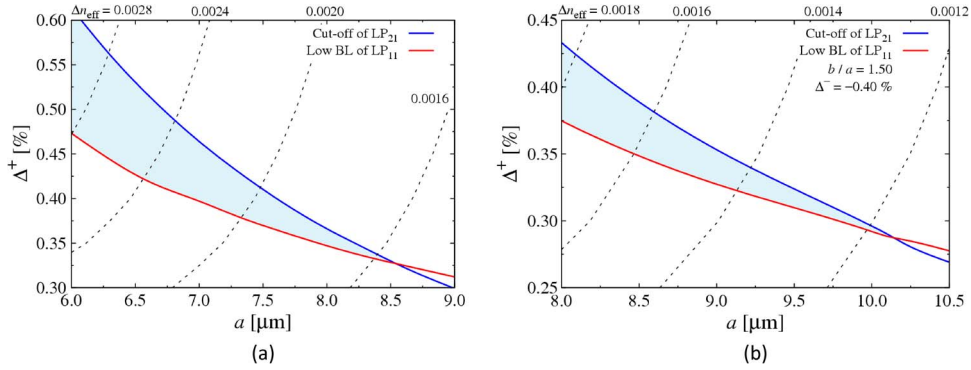


Fig. 5. Structural parameter dependence of $\Delta n_{\text{eff}}$ between $LP_{01}$ and $LP_{11}$ modes in two-mode (a) SIF and (b) WIF.

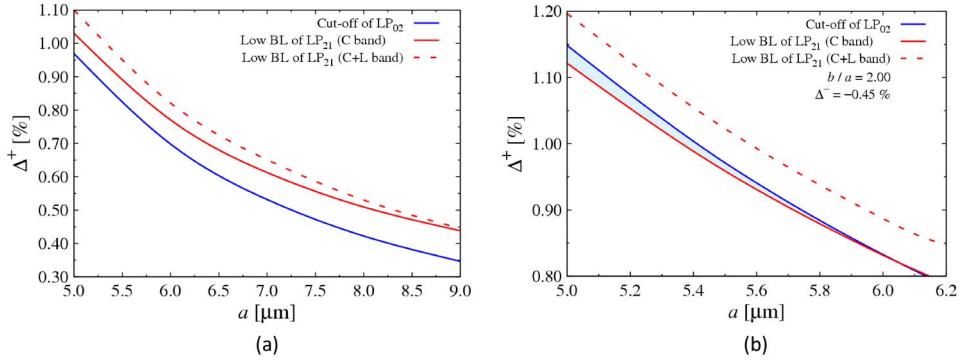


Fig. 6. Structural parameter dependence of design conditions in three-mode (a) SIF and (b) WIF.

1530 nm when the bending radius equals 140 mm. The low BL of $LP_{21}$ means that the BL of $LP_{21}$ mode is less than 0.5 dB/100 turns at 1565 nm or 1625 nm when the bending radius equals 30 mm.

Fig. 6 shows structural parameter dependence of design conditions in three-mode (a) SIF and (b) WIF with $b/a = 2.00$ and $\Delta^- = -0.45\%$. The solid blue curve indicates the upper limit of the BL of $LP_{02}$ mode and the solid and dashed red curves indicate the lower limits of the BL of $LP_{21}$ mode at 1565 nm and 1625 nm, respectively. From Fig. 6(a), we find that the structure satisfying the design conditions does not exist in three-mode SIF. This is because there is not much difference of the propagation constants between $LP_{21}$ and $LP_{02}$ modes in SIF. Therefore, the difference of the BL between them also becomes small and cannot satisfy the design conditions. As a solution, we employ WIF. From Fig. 6(b), it is evident that a WIF structure satisfying the design conditions over C band exists.

### 4.2. Limit of $A_{\text{eff}}$ Enlargement

We evaluate the limits of $A_{\text{eff}}$ enlargement in three-mode WIF over C band. Fig. 7(a) shows structural parameter to satisfy design conditions for three-mode WIF. The solid lines indicate the upper limits of the core radius $a$. The dashed lines indicate the lower limits of $\Delta^+$. From Fig. 7(a), we find that the core radius becomes maximum when we fix $b/a = 2.25$. Fig. 7(b) shows max $A_{\text{eff}}$ of $LP_{01}$, $LP_{11}$, and $LP_{21}$ modes at 1550 nm as a function of $b/a$ in three-mode WIF. The solid, dashed and one dashed-dot lines indicate the maximum $A_{\text{eff}}$ of $LP_{01}$, $LP_{11}$, and $LP_{21}$ modes, respectively. From Fig. 8(a) and (b), when the structural parameters are set to $b/a = 2.25$, $\Delta^- = -0.50\%$, $a = 6.3$ $\mu$m, and $\Delta^+ = 0.76\%$, the limits of $A_{\text{eff}}$ enlargement of the $LP_{01}$, $LP_{11}$, and $LP_{21}$ modes are 83 $\mu m^2$, 117 $\mu m^2$, 125 $\mu m^2$, respectively. The maximum $A_{\text{eff}}$ of $LP_{01}$ mode is similar to that of conventional SIF. Further enlargement of $A_{\text{eff}}$ in three-mode fiber is the subject for future analysis.

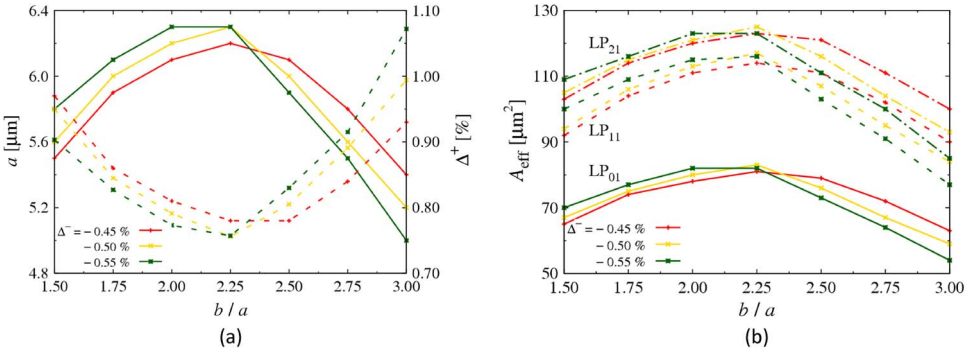


Fig. 7. (a) Structural parameter to satisfy design conditions for three-mode WIF. (b) Max $A_{\text{eff}}$ of $LP_{01}$, $LP_{11}$ and $LP_{21}$ modes at 1550 nm.

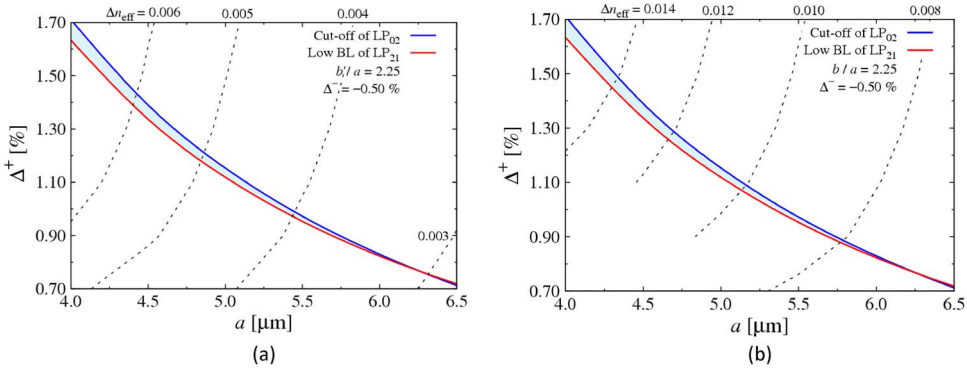


Fig. 8. Structural parameter dependence of $\Delta n_{\text{eff}}$ (a) between $LP_{01}$ and $LP_{11}$ modes and (b) between $LP_{11}$ and $LP_{21}$ modes in three-mode WIF.

### 4.3. Effective Index Difference $\Delta n_{\text{eff}}$

In three-mode transmission, we need to evaluate the $\Delta n_{\text{eff}}$ between each propagation modes. Fig. 8 shows variation of $\Delta n_{\text{eff}}$ at 1550 nm (a) between $LP_{01}$ and $LP_{11}$ modes, (b) between $LP_{11}$ and $LP_{21}$ modes in three-mode WIF with $b/a = 2.25$ and $\Delta^- = -0.50\%$ as a function of the core radius $a$ and $\Delta^+$. The solid blue and red curves are defined as before. From Fig. 8(a) and (b), we can see that the $\Delta n_{\text{eff}}$ in three-mode WIF between each propagation modes are more than approximately 0.003, 0.008, respectively. In contrast, the DMD of SIF and WIF are quit larger than that of graded-index fiber, which may result in requiring higher DSP complexity at the MIMO equalizers when we compensate for the mode crosstalk occurred at a mode-multiplexer/demultiplexer or splice points. However, Ref. [17] proposes an MDM system with reduced complexity MIMO processing, whose computational complexity is independent of the DMD value of the fiber. Therefore, we believe that DSP complexity can be kept low even with high DMD fibers such as SIF and WIF, when adopting the equalizer described in [17].

## 5. Conclusion

The region satisfying design conditions for two- or three-mode transmission has been investigated. We have also evaluated the limits of $A_{\text{eff}}$ enlargement and the $\Delta n_{\text{eff}}$ between propagation modes in two-mode SIF, two-mode WIF, and three-mode WIF. Through detailed numerical simulations, we found that the $A_{\text{eff}}$ larger than 200 $\mu m^2$ can be realized for both modes in two-mode WIF. Additionally, we have also clarified that three-mode SIF cannot meet design conditions, but WIFs satisfy three-mode transmission condition. Furthermore, by adopting other structures, enlargement of the region satisfying three-mode transmission condition is the subject for future analysis.

## References


[1] N. Hanzawa, K. Saitoh, T. Sakamoto, T. Matsui, S. Tomita, and M. Koshiba, "Demonstration of mode-division multiplexing transmission over 10 km two-mode fiber with mode coupler," presented at the OFC/NFOEC, Los Angeles, CA, USA, 2011, Paper OWA4.

[2] M. Salsi, C. Koebele, G. Charlet, and S. Bigo, "Mode division multiplexed transmission with a weakly-coupled few-mode fiber," presented at the OFC/NFOEC, Los Angeles, CA, USA, 2012, Paper OTU2C.5.

[3] R. Ryf, S. Randel, N. K. Fontaine, M. Montoliu, E. Burrows, S. Corteslli, S. Chandrasekhar, A. H. Gnauck, C. Xie, R.-J. Essiambre, P. J. Winzer, R. Delbue, P. Pupalaikis, A. Sureka, Y. Sun, L. Gruner-Nielsen, R. V. Jensen, and R. Lingle, "32-bit/s/Hz spectral efficiency WDM transmission over 177-km few-mode-fiber," presented at the OFC/NFOEC, Anaheim, CA, USA, 2013, Paper PDP5A.1.

[4] E. Ip, M. J. Li, K. Bennett, Y. K. Huang, A. Tanaka, A. Korolev, K. Koreshkov, W. Wood, E. Mateo, J. Hu, and Y. Yano, "146 $\times$ 6 $\times$ 19-Gbaud wavelength-and-mode-division multiplexed transmission over 10 $\times$ 50-km spans of few-mode fiber with a gain-equalized few-mode EDFA," presented at the OFC/NFOEC, Anaheim, CA, USA, 2013, Paper PDP5A.2.

[5] K. Mukasa, K. Imamura, R. Sugizaki, and T. Yagi, "Comparisons of merits on wide-band transmission systems between using extremely improved solid SMFs with $A_{\text{eff}}$ of 160 $\mu$m$^2$ and loss of 0.175 dB/km and using large-$A_{\text{eff}}$ holey fibers enabling transmission over 600 nm bandwidth," presented at the OFC/NFOEC, San Diego, CA, USA, 2008, Paper OThR1.

[6] T. Matsui, T. Sakamoto, K. Tsujikawa, S. Tomita, and M. Tsubokawa, "Single-mode photonic crystal fiber design with ultralarge effective area and low bending loss for ultrahigh-speed WDM transmission," *J. Lightw. Technol.*, vol. 29, no. 4, pp. 511–515, Feb. 2011.

[7] F. Ferreira, D. Fonseca, and H. Silva, "Design of few-mode fibers with arbitrary and flattened differential mode delay," *IEEE Photon. Technol. Lett.*, vol. 25, no. 5, pp. 438–441, Mar. 2013.

[8] L. Gruner-Nielsen, Y. Sun, J. Nicholson, D. Jakobsen, K. Jespersen, R. Lingle, and B. Palsdottir, "Few mode transmission fiber with low DGD, low mode coupling, and low loss," *J. Lightw. Technol.*, vol. 30, no. 23, pp. 3693–3698, Dec. 2012.

[9] P. Sillard, M. Bigot-Astruc, D. Boivin, H. Maerten, and L. Provost, "Few-mode fiber for uncoupled mode-division multiplexing transmissions," presented at the ECOC, Geneva, Switzerland, 2011, Paper Tu.5.LeCervin.7.

[10] K. Saitoh and M. Koshiba, "Full-vectorial imaginary-distance beam propagation method based on a finite element scheme: Application to photonic crystal fibers," *IEEE J. Quantum Electron.*, vol. 38, no. 7, pp. 927–933, Jul. 2002.

[11] *Characteristics of a Cut-Off Shifted, Single-Mode Fibre and Cable*, ITU-T Std. G.654, Oct. 2012.

[12] M. Bigot-Astruc, L. Provost, G. Krabshuis, P. Dhenry, and P. Sillard, "125 $\mu$m glass diameter single-mode fiber with $A_{\text{eff}}$ of 155 $\mu$m$^2$," presented at the OFC/NFOEC, Los Angeles, CA, USA, 2011, Paper OTuJ2.

[13] Y. Tsuchida, K. Mukasa, and R. Sugizaki, "Analyzing anew mechanism of air holes to suppress micro-bending loss," presented at the OFC/NFOEC, Los Angeles, CA, USA, 2012, Paper JW2A.19.

[14] C. Koebele, M. Salsi, G. Charlet, and S. Bigo, "Nonlinear effects in mode-division-multiplexed transmission over few-mode optical fiber," *IEEE Photon. Technol. Lett.*, vol. 23, no. 18, pp. 1316–1318, Sep. 2011.

[15] K. Jespersen, Z. Li, L. Gruner-Nielsen, B. Palsdottir, F. Poletti, and J. W. Nicholson, "Measuring distributed mode scattering in long few-moded fibers," presented at the OFC/NFOEC, Los Angeles, CA, USA, 2012, Paper OTh3I.4.

[16] L. Gruner-Nielsen, Y. Sun, J. W. Nicholson, D. Jakobsen, K. G. Jespersen, R. Lingle, and B. Palsdottir, "Few mode transmission fiber with low DGD, low mode coupling, and low loss," *J. Lightw. Technol.*, vol. 30, no. 23, pp. 3693–3698, Dec. 2012.

[17] T. Sakamoto, T. Mori, T. Yamamoto, N. Hanzawa, S. Tomita, F. Yamamoto, K. Saitoh, and M. Koshiba, "Mode-division multiplexing transmission system with DMD-independent low complexity MIMO processing," *J. Lightw. Technol.*, vol. 31, no. 13, pp. 2192–2199, Jul. 2013.